3D Bilayer Silicon Metasurface with Rhombus-arranged Air Holes (12/18/2024 updated)

To address the limitations of 2D gratings in polarization sensitivity and anisotropy, rhombus-arranged air holes are incorporated into silicon bilayer slabs. Additionally, the tunability method is simplified by adjusting the air gap alone, eliminating the need for liquid crystals.

Leveraging the versatile reconfigurability of flat photonics, this paper introduces a bilayer metasurface structure capable of achieving multiple filtering functionalities at a single operating wavelength, shown in Figure 5. Specifically, through tunning the air gap between two layers, the device can achieve switching between 40-degree FOV 2D edge detection and 40-degree FOV 2D center blur & denoising via air gap tunning with unpolarized light source and high isotropy. This work is among the first to achieve such a functional switch using flat photonics, laying the foundation in computational metasurfaces to perform multi-order derivative operations for imaging applications.

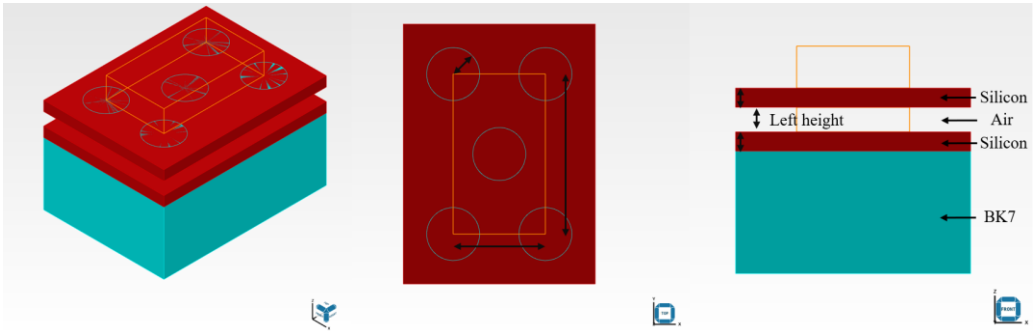

Figure 5 Schematic Diagram. Bilayer silicon transmissive metasurface with rhombus-arranged air holes, presented in three perspectives: 3D view, top view, and side view, displayed from left to right. The angle between each air hole is 60 degree. Through tunning left air gap height, it can achieve different filtering functionalities.

To achieve edge detection of the input image, the metasurface's transfer function must strongly suppress the central spatial frequencies in the Fourier-transformed input image while allowing high transmission of other spatial frequencies. In contrast, center blur operates by performing the opposite effect. Thus, it is essential to design a transmissive, reconfigurable metasurface whose transfer function can be adjusted through specific tuning techniques to meet the requirements for both edge detection and center blur. Based on the pervious edge detection metasurface, the metasurface is firstly split into bilayer to introduce air gap tunning, and Figure 6 (Left for s-pol input s-pol detect, Right for p-pol input p-pol detect) sweeping the spectrum across the incident angle.

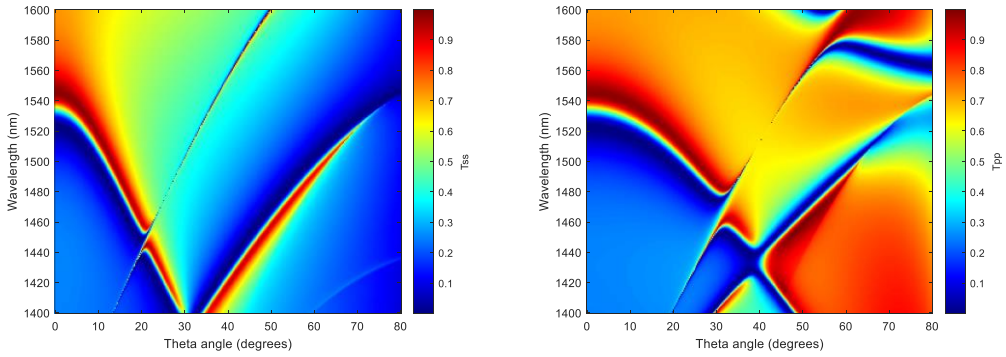

Figure 6 Incident θ Angle Sweeping Spectrum @ $\phi = 0°$: (Left) Transmission of s-pol with s-pol input with certain initial air gap (Right) Transmission of p-pol with p-pol input

This result defined the initial edge detection condition, where at normal incident the transfer function can suppress the spatial signal to <0.1 level, and the device working wavelength (~1520nm). Through Azimuthal angle sweeping, Figure 7 (a, b) shows the transfer function of the metasurface with p-pol input p-pol detect and s-pol input s-pol detect for edge detection.

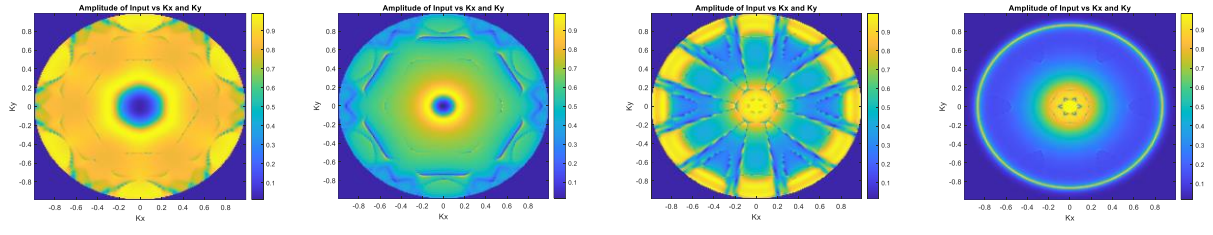

(a) (b) (c) (d)

Figure 7 Metasurface Transfer Function @ NA 80°: (a,c) Transmission of p-pol with p-pol input, (b,d) Transmission of s-pol with s-pol input

To expand the functionality to center blur, the left gap sweeping is necessary, shown in Figure 8. It achieves center blur & denoising at larger left height under the same working wavelength, which is based on the cavity resonance of the bilayer. Figure 7 (c, d) shows the transfer function with p-pol input p-pol detect and s-pol input s-pol detect of the metasurface for center blur.

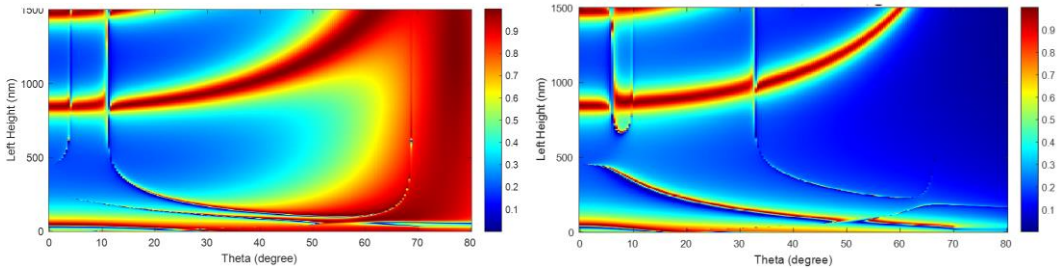

Figure 8 Angle Spectrum with left height @ $\phi = 0°$: (Left) Transmission of p-pol with p-pol input, (Right) Transmission of s-pol with s-pol input

Based on the switch of transfer function via gap tunning, initially our fourier calculation shows that the metasurface is capable of 2D edge detection and 1D center blur & denoising (12/01 result). After further investigation, the functionalities have updated. The metasurface can achieve the switch between 40-degree FOV 2D edge detection and 40-degree FOV 2D center blur & denoising via air gap tunning (12/18 updated) with high polarization insensitivity and high isotropy. It shows that the silicon air hold bilayer metasurface has strong reconfigurability in different spatial frequency filtering tasks. The test of Octagon Input Image is shown in Figure 9.a and b.

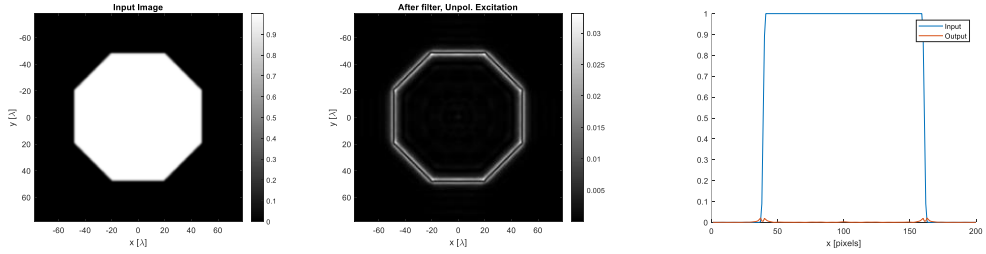

Figure 9.a. 2D Edge Detection Functionality Plots (40 degree FOV): From left to right, unpolarized input octagon image, output after metasurface with certain air gap at one wavelength, x-cross section of output

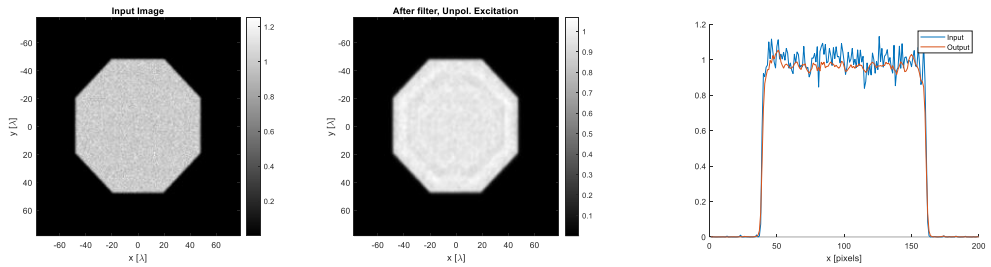

Figure 9.b. 2D Center Blur & Denoising Functionality Plots (40 degree FOV): From left to right, unpolarized input octagon image with $\delta = 0.001$ noise, output after metasurface with a different air gap at the same wavelength, x-cross section of output

The metasurface can achieve the switch between these two functionalities with air gap tunning. The target air gap difference of these two functionalities has a large difference (~1450nm) which makes the device less sensitive to mechanical tunning error. In the Figure 9.b, after the metasurface, the initial variance in the input image reduces to ~10% and at the edge there is the effect of center blur. In addition, for the edge detection, the reason the output edge has low efficiency is the metasurface has filtered out the intensity concentrated center spatial frequency. And for the center blur, the output image still has relatively high efficiency showing the metasurface has relatively low loss for center blur.

This work is among the first to achieve a switch between multifunctionality in Fourier Frequency Filtering using the same device and operating at the same wavelength with high polarization insensitivity and isotropy. Beyond imaging metasurfaces, it establishes a valuable foundation for reconfigurable computational metasurfaces capable of performing multi-order derivative operations on signals.